

PAPER • OPEN ACCESS

Thermodynamics and optimal protocols of multidimensional quadratic Brownian systems

To cite this article: Paolo Abiuso *et al* 2022 *J. Phys. Commun.* **6** 063001

View the [article online](#) for updates and enhancements.

You may also like

- [Underdamped stochastic heat engine at maximum efficiency](#)
A. Dechant, N. Kiesel and E. Lutz
- [Efficient protocols for Stirling heat engines at the micro-scale](#)
Paolo Muratore-Ginanneschi and Kay Schwieger
- [Optimally robust shortcuts to population inversion in two-level quantum systems](#)
A Ruschhaupt, Xi Chen, D Alonso et al.



PAPER

OPEN ACCESS

RECEIVED

10 March 2022

REVISED

19 May 2022

ACCEPTED FOR PUBLICATION

24 May 2022

PUBLISHED

13 June 2022

Original content from this work may be used under the terms of the [Creative Commons Attribution 4.0 licence](https://creativecommons.org/licenses/by/4.0/).

Any further distribution of this work must maintain attribution to the author(s) and the title of the work, journal citation and DOI.



Thermodynamics and optimal protocols of multidimensional quadratic Brownian systems

Paolo Abiuso^{1,2} , Viktor Holubec³ , Janet Anders^{4,5}, Zhuolin Ye⁶, Federico Cerisola^{4,7} and Martí Perarnau-Llobet²

¹ ICFO-Institut de Ciències Fotòniques, The Barcelona Institute of Science and Technology, 08860 Castelldefels (Barcelona), Spain

² Department of Applied Physics, University of Geneva, 1211 Geneva, Switzerland

³ Charles University, Faculty of Mathematics and Physics, Department of Macromolecular Physics, V Holešovičkách 2, CZ-180 00 Praha, Czech Republic

⁴ Department of Physics and Astronomy, University of Exeter, Stocker Road, Exeter EX4 4QL, United Kingdom

⁵ Institut für Physik und Astronomie, University of Potsdam, 14476 Potsdam, Germany

⁶ Institut für Theoretische Physik, Universität Leipzig, Postfach 100 920, D-04009 Leipzig, Germany

⁷ Department of Materials, University of Oxford, Parks Road, Oxford OX1 3PH, United Kingdom

E-mail: paolo.abiuso@icfo.eu

Keywords: stochastic thermodynamics, thermodynamic control, thermodynamic length, overdamped brownian systems

Abstract

We characterize finite-time thermodynamic processes of multidimensional quadratic overdamped systems. Analytic expressions are provided for heat, work, and dissipation for any evolution of the system covariance matrix. The Bures-Wasserstein metric between covariance matrices naturally emerges as the local quantifier of dissipation. General principles of how to apply these geometric tools to identify optimal protocols are discussed. Focusing on the relevant slow-driving limit, we show how these results can be used to analyze cases in which the experimental control over the system is partial.

1. Introduction

The minimisation of dissipation is a central goal in finite-time thermodynamics [1–3]. In most applications, one is interested in finding the optimal time variation of some control parameters, e.g., magnetic or electric fields, in order to achieve a desired task while minimising the amount of energy dissipated to the environment. Such tasks could range from the design of a cycle for a thermal engine [4, 5] to the erasure of information in an information processing device [6–8]. Finding optimal protocols in finite time is however often a very challenging task, as it requires a functional optimisation over all possible paths in the control parameter space, as well as a perfect understanding of the non-equilibrium dynamics resulting from such control. In the regime of small mesoscopic systems, remarkable progress on this topic has been achieved in the last decades with the development of the field of stochastic thermodynamics [4, 9–14]. Optimal drivings are nowadays known for overdamped [15–20] and underdamped systems [21–23], as well as driven single-level quantum dots [24]. However, such explicit solutions only exist for one-dimensional systems and are, in general, computationally hard to scale up.

Other solutions are known for situations in which the control parameter varies *slowly* compared to the system relaxation time, as the optimisation admits a geometric formulation [25–32] and the problem considerably simplifies. Indeed, the space of control parameters can be endowed with a Riemannian metric in such a way that geodesic paths correspond to minimally dissipative thermodynamic processes. While the geodesic equations might be hard to solve, the important realisation is that the number of coupled equations is given by the number of control parameters, and independent of the size of the system of interest (by comparison, a full out-of-equilibrium solution of the dynamics needs a number of equations that scales exponentially with the number of components of the system). This has enabled finding optimal driving protocols in such regime for complex systems such as a two dimensional Ising model [33, 34], nanomagnets [35], and quantum spin chains [36]. Optimal protocols for different classes of slowly driven heat engines have also been developed by such a

geometric approach [32, 37–44]. Besides the slow driving regime, the optimization problem can also be simplified in the opposite, *fast-driving*, regime [45–48].

Beyond the slow or fast driving limits, a general connection has been established between optimal transport and minimally-dissipative thermodynamic protocols in the overdamped limit [49, 50]. This connection was recently exploited to show that the minimal dissipation in any process governed by a Langevin equation is directly related to the L^2 -Wasserstein distance between initial and final states [51, 52] (see also [53–55]). However in general full control on the system's Hamiltonian is needed to saturate this bound. To address the relevant case of partial experimental control, one therefore requires a different approach, that is able to quantify dissipation on non-optimal trajectories.

In this paper, we study thermodynamic transformations for many-body quadratic overdamped systems. We derive general expressions for the flux of work and heat, and we show that the dissipation is governed by the Bures-Wasserstein (BW) distance between covariance matrices, which coincides with the L^2 -Wasserstein distance between Gaussian distributions of [51–55]. Our derivation allows for a direct generalisation of the well-known single-body case, studied by Schmiedl and Seifert for a single-particle overdamped system [15], as well as new insights on the form of optimal drivings. In particular, we provide an integral analytic expression for the dissipation valid for *any response trajectory* of the system, not necessarily minimally dissipating. This also naturally enables the study of *partial control*. That is, the situation where the limited number of control parameters does not allow for exploring the whole space of states, so that the fundamental lower bounds of [49, 51] might not be reachable. This is a common scenario in complex systems, where experimentally only a few degrees of freedom are controllable. In order to illustrate the applicability of our results, and to show the difference between partial and global control, we analyse a system of two interacting particles and a particle confined in a 2-dimensional squeezing potential with different control limitations.

2. Model: Many-body overdamped spring

We consider a system of N overdamped Brownian particles described by the position vector \mathbf{x} and mutually interacting via the time-dependent potential

$$V(\mathbf{x}, t) = \frac{1}{2} \mathbf{x}^\top K(t) \mathbf{x}, \quad (1)$$

or, equivalently, via the force field $F(\mathbf{x}) = -\nabla V(\mathbf{x}) = -K\mathbf{x}$ (when possible, we omit writing the time argument from now on). Each particle $i = 1, \dots, N$ might have a different number of degrees of freedom d_i , i.e., $\mathbf{x} \in \mathbb{R}^M$, where $M = \sum_{i=1}^N d_i$. The potential (1) accounts for both self-energy of the individual particles and interactions between the particles. The stiffness matrix K is symmetric and positive definite $K \geq 0$ (that is, the potential is confining). Assuming that all the particles have the same friction coefficient γ , the system dynamics obeys the set of Langevin equations [56]

$$\gamma \dot{\mathbf{x}} = -K\mathbf{x} + \sqrt{2\gamma k_B T} \boldsymbol{\eta}, \quad (2)$$

where the Gaussian noise $\boldsymbol{\eta}$ obeys $\langle \boldsymbol{\eta} \rangle = 0$, its components $\langle \eta_i(t) \eta_j(t') \rangle = \delta_{ij} \delta(t - t')$, and T is the temperature of the thermal environment, which we assume is fixed throughout (isothermal). From now on, we will use natural units in which $\gamma = 1$, $k_B = 1$. For the general case in which different particles have different friction coefficients, see section 4.

Departing from an arbitrary normalized initial distribution, the state of the system at time t is represented by a Gaussian probability density function (PDF) [56]⁸.

$$p(\mathbf{x}, t) = \frac{1}{\sqrt{(2\pi)^N \det \Sigma}} \exp\left(-\frac{\mathbf{x}^\top \Sigma^{-1}(t) \mathbf{x}}{2}\right). \quad (3)$$

Here $\Sigma(t) = \langle \mathbf{x} \mathbf{x}^\top \rangle(t)$ denotes the covariance matrix at time t . The PDF (3) has zero mean $\langle \mathbf{x} \rangle(t) = 0$ (see section 4 and appendix B for the more general case).

The distribution $p(\mathbf{x}, t)$ is therefore defined by its covariance matrix, whose dynamics $\dot{\Sigma} = \langle \dot{\mathbf{x}} \mathbf{x}^\top \rangle + \langle \mathbf{x} \dot{\mathbf{x}}^\top \rangle$ can be obtained from equation (2) and reads [56]

$$\dot{\Sigma}(t) = -K(t)\Sigma(t) - \Sigma(t)K(t) + 2T, \quad (4)$$

where implicitly $T = T1$. In case the response dynamics $\Sigma(t)$ is given, and one wants to drive the potential $K(t)$ accordingly (i.e., $K(t)$ is the control protocol generating the response dynamics $\Sigma(t)$), the above equation has to be solved for $K(t)$. This is a standard Lyapunov equation that is commonly used in the context of quantum

⁸ The PDF describing the state under the dynamics (2) is always Gaussian given Gaussian initial conditions, or after an initial transient (of order $\gamma/|K|$) [56] which is negligible for standard time-asymptotic cycling scenarios, or in the regime of slow driving.

metrology (see e.g., [57]), having solution

$$K = \int_0^\infty d\nu e^{-\nu\Sigma} (2T - \dot{\Sigma}) e^{-\nu\Sigma} = T\Sigma^{-1} - \int_0^\infty d\nu e^{-\nu\Sigma} \dot{\Sigma} e^{-\nu\Sigma}. \quad (5)$$

Notice that instantaneous quenches of $K(t)$ can be added at the beginning and at the end of the protocol, without affecting the dynamics of $\Sigma(t)$. For example, to end the transformation in equilibrium, one can add a final quench to $K = T\Sigma^{-1}$.

Remark. We stress here that the explicit evaluation of equation (5) can be performed analytically. To be consistent with the notation, throughout the text we use the operator $\mathcal{I}(A, B) = \int_0^\infty d\nu e^{-\nu A} B e^{-\nu A}$ expressed in its integral matrix form; at the same time, in the basis that diagonalizes A , i.e., $A_{ij} = \delta_{ij} a_i$, the components of this operator can be easily expressed as $\mathcal{I}(A, B)_{ij} = \frac{B_{ij}}{a_i + a_j}$.

3. Thermodynamics of quadratic systems

The average energy of a system described by a multidimensional probability distribution (3) in the potential (1) reads

$$E(t) = \int d\mathbf{x} p(\mathbf{x}, t) V(\mathbf{x}, t) = \sum_{ij} \frac{1}{2} K_{ij}(t) \langle x_i x_j \rangle(t) = \frac{\text{Tr}[K(t)\Sigma(t)]}{2}, \quad (6)$$

where $\text{Tr}[AB] = \sum_{ij} A_{ij} B_{ji}$. The variation of energy is split canonically in a work contribution, originating in the variation of the external potential, and a heat contribution, stemming from the evolution of the system induced by the dissipative environment [4, 58]. I.e. the work (W) and heat (Q) fluxes entering the system are defined as

$$\dot{W} = \frac{\text{Tr}[\dot{K}\Sigma]}{2}, \quad \dot{Q} = \frac{\text{Tr}[K\dot{\Sigma}]}{2}. \quad (7)$$

In a similar fashion to the seminal work by Schmiedl and Seifert [15] we can write the work input of a finite time transformation of duration τ as

$$\begin{aligned} W &= \frac{1}{2} \int_0^\tau dt \text{Tr}[\dot{K}\Sigma] \\ &= \frac{1}{2} \text{Tr}[K\Sigma] \Big|_0^\tau - \frac{T}{2} \log \det \Sigma \Big|_0^\tau + \frac{1}{2} \int_0^\tau dt \text{Tr} \left[\int_0^\infty d\nu e^{-\nu\Sigma} \dot{\Sigma} e^{-\nu\Sigma} \right], \end{aligned} \quad (8)$$

where in the second equality we integrated by parts and used equation (5). In the following we will indicate as $\mathcal{Q}(\tau) - \mathcal{Q}(0) := \Delta \mathcal{Q}$ the variation of any quantity \mathcal{Q} during a transformation. Given that $\frac{1}{2} \log \det \Sigma \Big|_0^\tau = - \int d\mathbf{x} p \ln p \Big|_0^\tau = \Delta S$ is the variation of Von Neumann entropy of the system (3), it is possible to rewrite equation (8) as

$$W - (\Delta E - T\Delta S) = \frac{1}{2} \int_0^\tau dt \text{Tr} \left[\int_0^\infty d\nu e^{-\nu\Sigma} \dot{\Sigma} e^{-\nu\Sigma} \right] \equiv W_{\text{irr}}. \quad (9)$$

This expression identifies the dissipated work, W_{irr} , of an arbitrary response trajectory $\Sigma(t)$. This is our first main result. The above derivation represents a natural multidimensional generalisation of the one-dimensional result of [15].

The irreversible work (9) turns out to be the integral in time of a quadratic form that coincides with the Bures-Wasserstein (BW) metric on positive-definite matrices [59, 60]. That is $W_{\text{irr}} = \int_0^\tau dt g_\Sigma(\dot{\Sigma}, \dot{\Sigma})$, where

$$g_\Sigma(A, B) = \frac{1}{2} \int_0^\infty d\nu \text{Tr}[e^{-\nu\Sigma} A e^{-\nu\Sigma} B], \quad (10)$$

$$g_\Sigma(d\Sigma, d\Sigma) \equiv D_{\text{BW}}(\Sigma, \Sigma + d\Sigma)^2, \quad (11)$$

with the latter being the infinitesimal BW squared distance. This metric has been intensely studied as it appears in problems of statistical inference and metrology in quantum information [57, 59, 61, 62], as well as in the theory of optimal transport [60, 63].

For fixed endpoints, the lower bound for W_{irr} is obtained for the response trajectory $\bar{\Sigma}(t)$ that minimizes the integral of the quadratic form in equation (9). That is

$$W_{\text{irr}} \geq \frac{D_{\text{BW}}(\Sigma_1, \Sigma_2)^2}{\tau}, \quad (12)$$

where the BW-geodesic length between the initial and final points $\Sigma(0) = \Sigma_1, \Sigma(\tau) = \Sigma_2$, is given by (see appendix A, or [59, 60])

$$D_{\text{BW}}(\Sigma_1, \Sigma_2)^2 \equiv \text{Tr}[\Sigma_1] + \text{Tr}[\Sigma_2] - 2 \text{Tr}[\sqrt{\sqrt{\Sigma_1} \Sigma_2 \sqrt{\Sigma_1}}]. \tag{13}$$

The corresponding geodesic, i.e., the minimally dissipating response trajectory, is given by (cf appendix A)

$$\bar{\Sigma}(s\tau) = (1 - s)^2 \Sigma_1 + s^2 \Sigma_2 + s(1 - s)(\sqrt{\Sigma_1 \Sigma_2} + \sqrt{\Sigma_2 \Sigma_1}), \tag{14}$$

with $s = t/\tau$ and thus $0 \leq s \leq 1$ independently on the total duration t of the protocol.

The appearance of the distance (13) in (12) is no coincidence: it was realised recently [51, 52] that the optimal transport problem is connected to the irreversible entropy production in diffusive dynamics, and its value is minimized by the L^2 -Wasserstein distance between the initial and final distributions [49, 51, 52, 64]. In the case of Gaussian distributions, the L^2 -Wasserstein distance coincides with the above BW distance between the covariance matrices (13).

Besides it being straightforward, one key advantage of our derivation is that expression (9) is valid for *any* response trajectory and allows to compute W_{irr} also when the transformation does not saturate the lower bound (12). In particular, it can be used for the realistic case of partial experimental control, when the system is constrained to explore only a subset of the distributions space (see the following paragraph and examples in section 5).

3.1. Total control versus partial control

In experiments, the system is typically controlled by varying $K(t)$. The optimal control parameter protocol \bar{K} corresponding to the geodesic (14) is determined by substituting $\bar{\Sigma}$ into (5). Perfect implementation of \bar{K} would then saturate the minimal dissipation bound (13). However, this assumes that \bar{K} is experimentally feasible. This might not be the case in general. Performing the minimization over a restricted region of control parameters limits the system response to a submanifold of allowed states. In general, this results in a case-dependent minimum value strictly larger than the global minimum, $W_{\text{irr}} > D_{\text{BW}}^2/\tau$, e.g., see Example 5.1 below.

In other cases, the initial and final point of the transformation might not even be fixed (e.g., when optimizing the strokes of a thermal cycle to increase its performance as a heat engine). To show the consequences of fixed/unfixed boundary states $\Sigma(0)$ and $\Sigma(\tau)$, consider that the variation $\dot{\Sigma} = \dot{\Sigma}_d + \dot{\Sigma}_r$ can be divided into a diagonal contribution and a non-diagonal, *rotating* contribution. That is, given the covariance matrix expressed in its diagonal basis $\Sigma = \sum_i \omega_i |i\rangle \langle i|$, the diagonal part of its variation is $\dot{\Sigma}_d = \sum_i \dot{\omega}_i |i\rangle \langle i|$ and the rotating part is $\dot{\Sigma}_r = \sum_i \omega_i (|\dot{i}\rangle \langle i| + |i\rangle \langle \dot{i}|)$. From equations (9) and (10) we know that $\dot{W}_{\text{irr}} = g_{\Sigma}(\dot{\Sigma}, \dot{\Sigma})$. It is easy to check that $g_{\Sigma}(\dot{\Sigma}_d, \dot{\Sigma}_r) = 0$ which implies that the irreversible work naturally decouples into a diagonal and a rotating contribution:

$$\dot{W}_{\text{irr}} = g_{\Sigma}(\dot{\Sigma}_d, \dot{\Sigma}_d) + g_{\Sigma}(\dot{\Sigma}_r, \dot{\Sigma}_r) \equiv \dot{W}_{\text{irr}}^{(d)} + \dot{W}_{\text{irr}}^{(r)}. \tag{15}$$

Both $\dot{W}_{\text{irr}}^{(d)}$ and $\dot{W}_{\text{irr}}^{(r)}$ are positive, which means that the dissipation generated in a non-commuting transformation for Σ ($\dot{W}_{\text{irr}}^{(r)} > 0$) is always larger than the commuting case ($\dot{W}_{\text{irr}}^{(r)} = 0$). (A similar phenomenon occurs for quantum systems, described by their density matrices [32]). At the same time, for any transformation $\Sigma(t) = \sum_i \omega_i(t) |i(t)\rangle \langle i(t)|$, the change in system entropy $\propto \Delta[\log \text{det} \Sigma]$ and energy $\propto \Delta[\text{Tr}[K \Sigma]]$ can also be achieved by a similar transformation $\Sigma^*(t) = \sum_i \omega_i(t) |i(0)\rangle \langle i(0)|$ (where $\omega_i(t)$ varies with time as in $\Sigma(t)$, while the basis is fixed) in which the covariance matrix commutes with itself at all times $[\Sigma^*(t), \Sigma^*(t')] = 0$, and $W_{\text{irr}}^{(r)} = 0$. Moreover, it is easy to verify that such transformation has the same value of $\dot{W}_{\text{irr}}^{(d)}$, which leads to the following observation:

Observation 1. If the restrictions on the control parameters $K(t)$ allow and $[\Sigma(0), \Sigma(\tau)] = 0$, rotation of the covariance matrix should be avoided in order to minimize dissipation.

In fact, it is clear that the BW-geodesic (14) is diagonal in the same basis at all times, if and only if $[\Sigma(0), \Sigma(\tau)] = 0$. If that is not the case, one cannot use $\Sigma^*(t)$ to reduce the dissipation, unless the endpoint of the trajectory is itself unconstrained. In the fully commuting case, it is easy to see that equations (6)–(9) simplify and we recover (K being diagonal in the same basis of Σ , with eigenvalues k_i)

$$E = \frac{1}{2} \sum_i k_i \omega_i, \quad \Delta S = \frac{1}{2} \sum_i \Delta[\log \omega_i],$$

$$W_{\text{irr}} = \int_0^\tau dt \sum_i \frac{1}{4} \frac{\dot{\omega}_i^2}{\omega_i} \geq \frac{1}{\tau} \sum_i (\sqrt{\omega_i(\tau)} - \sqrt{\omega_i(0)})^2. \tag{16}$$

When reduced to a single mode, this is exactly the result found by Schmiedl and Seifert in [15], which we thus see being *extensive in the eigenmodes* ω_i of Σ : that is, all the modes $\{\omega_i, k_i\}$ can be treated as effectively independent in the commuting case. As an instance of a transformation with fixed boundaries that force non-commutation, see Example 5.2.

As mentioned above, controlling the potential (1) in time defines the evolution of the state via the dynamical equation (4). Conversely, a given response trajectory $\Sigma(t)$ is translated to its generating control $K(t)$ through equation (5). This means that fixing the boundary values of Σ is non-trivially related to fixing boundary controls. The results of optimisation thus strongly depend on the imposed constraints [65, 66, 67]. At the same time, for the purpose of typical applications to isothermal processes (cf section 5), in which the goal is to minimize work dissipation, we can consider the *slow-driving* limit of the dynamics [68]. In this limit the potential $K(t)$ is modified slowly, more precisely we assume $\dot{K} \sim 1/\tau$ with τ much larger than the relaxation timescale of the system $\tau \gg \gamma/|K|$, and it is sufficient to solve the dynamical equation (4) up to the first order in $1/\tau$. The zeroth order corresponds to the quasistatic limit $\tau \rightarrow \infty$. This allows to expand any state-dependent quantity \mathcal{Q} around its equilibrium value $\mathcal{Q}^{(0)}$, keeping only the leading correction term $\mathcal{Q}^{(1)} \sim \mathcal{O}(1/\tau)$. In our specific setting, the covariance matrix can be expanded as

$$\Sigma(t) = \Sigma^{(0)}(t) + \Sigma^{(1)}(t) + \mathcal{O}(1/\tau^2) \quad (17)$$

with $\Sigma^{(0)} = TK^{-1}$ and $\Sigma^{(1)} = -T \int_0^\infty d\nu e^{-\nu/K} \frac{d}{dt}(K^{-1}) e^{-\nu/K}$ (cf equations (4) and (5)). However, the irreversible work (9) is already of order $\mathcal{O}(1/\tau)$. To express the dissipation in the slow regime, it is therefore sufficient to substitute $\Sigma^{(0)}$ in (9). In other words, we observe that

Observation 2. In the slow-driving limit, controlling the inverse stiffness matrix $TK^{-1}(t)$ of the potential is equivalent to directly steering the covariance matrix $\Sigma(t)$. The irreversible work in the slow-driving limit therefore reads

$$W_{\text{irr}}^{\text{slow}} = \frac{T}{2} \int_0^\tau dt g_{K^{-1}} \left(\frac{d}{dt}(K^{-1}), \frac{d}{dt}(K^{-1}) \right). \quad (18)$$

4. Generalizations

In the previous section, we have focused on the paradigmatic case of the potential (1) and density distributions (3) centered around $\mathbf{x} = 0$, and a particle-independent friction coefficient. Nevertheless, the obtained results are fully extendable also when removing such assumptions.

First, in appendix B we solve the general case of a quadratic potential with time-dependent center $\mathbf{z}(t)$, i.e., $V(\mathbf{x}, t) = \frac{1}{2}(\mathbf{x} - \mathbf{z}(t))K(t)(\mathbf{x} - \mathbf{z}(t))$. As the system is in general driven out of equilibrium, the center of the potential does not necessarily coincide with the average particle position, $\langle \mathbf{x} \rangle \equiv \boldsymbol{\xi}(t) \neq \mathbf{z}(t)$, and the irreversible work gains an additional contribution (see details in appendix B). Focusing on the limit of slow driving, it can be expressed as

$$W_{\text{irr}}^{\text{slow}} = \int_0^\tau dt (|\dot{\boldsymbol{\xi}}|^2 + g_\Sigma(\dot{\Sigma}, \dot{\Sigma})). \quad (19)$$

Similarly to (13), the lower bound for $W_{\text{irr}}^{\text{slow}}$ is in this case

$$W_{\text{irr}}^{\text{slow}} \geq \frac{1}{\tau} (|\boldsymbol{\xi}_1 - \boldsymbol{\xi}_2|^2 + D_{BW}(\Sigma_1, \Sigma_2)^2). \quad (20)$$

Observations 1 and 2 from section 3 remain valid: if possible, rotations of the covariance matrix thus should be avoided; the state variables in the expression (19) can be substituted by their equilibrium values $(\boldsymbol{\xi}, \Sigma) = (\mathbf{z}, TK^{-1})$. Moreover, in the same limit, $\boldsymbol{\xi}(t) - \mathbf{z}(t) \sim \mathcal{O}(\tau^{-1})$ while the associated correction to quasistatic ΔE and ΔS is negligible $\mathcal{O}(\tau^{-2})$ (cf appendix B). This implies that moving the trap $\dot{\boldsymbol{\xi}} \neq 0$ only contributes to the dissipation (20) and should therefore be avoided when possible, in the same spirit as Observation 1.

Second, we comment on the generalization to systems where different particles have different friction coefficients γ_i . In such a case, the Langevin equations (2) become, in components,

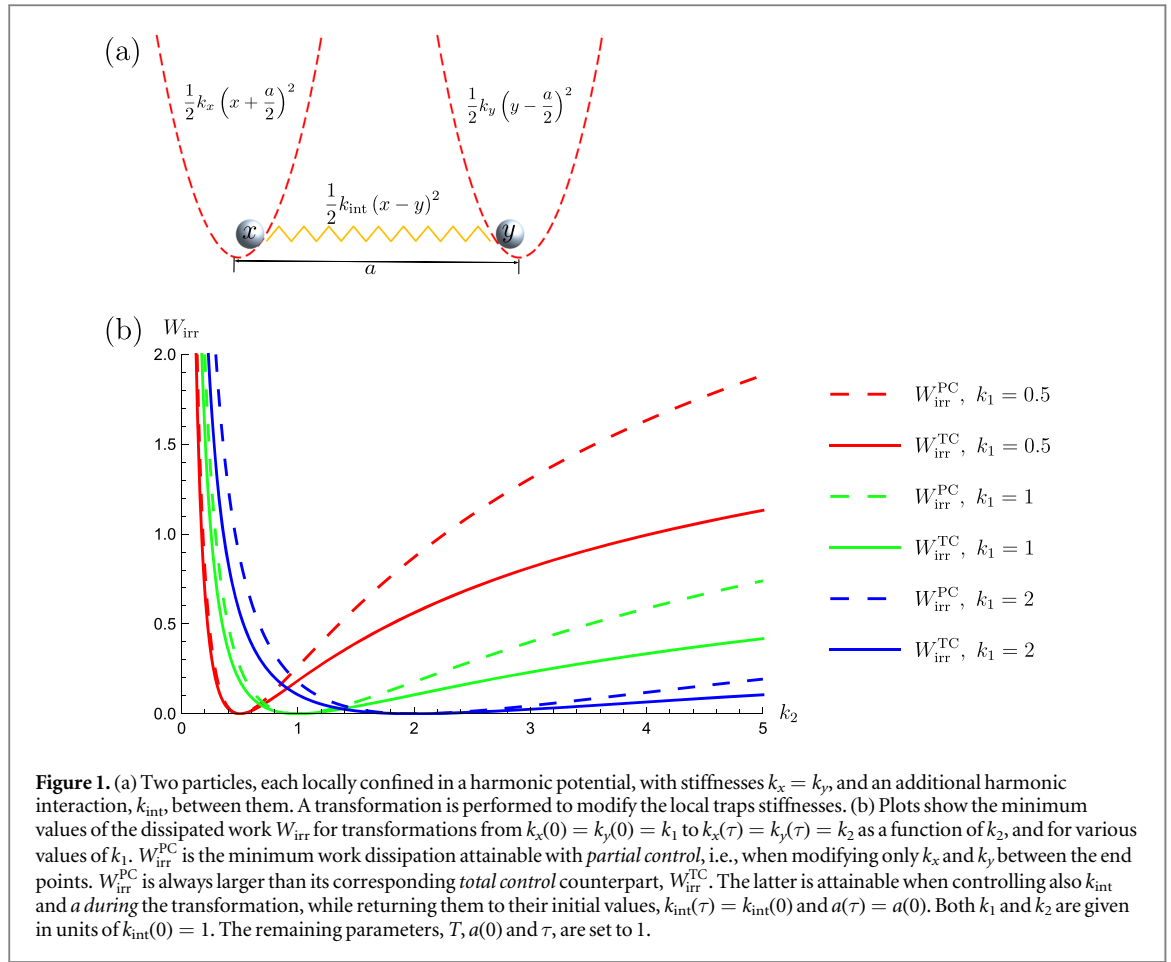
$$\gamma_i \dot{x}_i = -\sum_j K_{ij} x_j + \sqrt{2\gamma_i k_B T} \eta_i. \quad (21)$$

Notice that some of the γ_i might refer to different degrees of freedom of the same particle. The white noises η_i are mutually uncorrelated. We define $y_i \equiv \sqrt{\gamma_i} x_i$ and rewrite the Langevin equations as

$$\dot{\mathbf{y}} = -K' \mathbf{y} + \sqrt{2k_B T} \boldsymbol{\eta}, \quad (22)$$

where the transformed stiffness matrix $K'_{ij} = \frac{K_{ij}}{\sqrt{\gamma_i \gamma_j}}$ is still symmetric and positive definite. At the same time, the covariance matrix of the \mathbf{y} variable, $\Sigma' = \langle \mathbf{y} \mathbf{y}^\top \rangle$, satisfies $\Sigma'_{ij} = \sqrt{\gamma_i} \Sigma_{ij} \sqrt{\gamma_j}$. Finally the energy of the system is given by

$$E = \frac{1}{2} \text{Tr}[\Sigma K] = \frac{1}{2} \text{Tr}[\Sigma' K'], \quad (23)$$



and similarly $\dot{Q} = \frac{1}{2} \text{Tr}[\dot{\Sigma}'K']$ and $\dot{W} = \frac{1}{2} \text{Tr}[\Sigma'\dot{K}']$. Given the formal equivalence between equations (2), (6), (7) and (22), (23) above, we see that the problem is equivalently mapped to the case with fixed $\gamma_i = \gamma, \forall i$.

Finally, throughout the paper we assumed a fixed temperature T . At the same time, the expressions for energy (6), heat and work (7), as well as $\Delta S = \frac{1}{2} \Delta \log \det \Sigma$ do not intrinsically depend on the temperature T . We can therefore relax such assumption and admit a time-dependent temperature $T(t)$ [69, 70]. In such case the definition of irreversible work becomes

$$W_{\text{irr}} = W - \left(\Delta E - \int_0^\tau dt T \dot{S} \right) = -Q + \int_0^\tau dt T \dot{S} = \int_0^\tau dt T \dot{S}_{\text{irr}}, \tag{24}$$

\dot{S}_{irr} being the irreversible entropy production. From the derivation in section 3 we get the same expression $W_{\text{irr}} = \frac{1}{2} \int_0^\tau dt g_{\Sigma}(\dot{\Sigma}, \dot{\Sigma})$, as well as the validity of all the above observations and generalizations.

5. Applications

Here, we present two examples of application of the formalism, results and observations introduced above.

5.1. Interacting particles in double trap

First, we show how partial control over a system can substantially increase the amount of dissipation when compared to the optimal geodesics transformation. Consider the case of two particles on a line, *Romeo and Juliet*, who are constrained to be located at two different places, separated by a distance a . That is, Romeo (Juliet) is at position x (y) and subject to a confining harmonic potential of strength k_x (k_y) centered at $\frac{a}{2}$ ($-\frac{a}{2}$). At the same time, the two particles feel a harmonic attraction of strength k_{int} . The complete system is described by the potential (cf figure 1)

$$V = \frac{1}{2} k_x \left(x - \frac{a}{2} \right)^2 + \frac{1}{2} k_y \left(y + \frac{a}{2} \right)^2 + \frac{1}{2} k_{\text{int}} (x - y)^2, \tag{25}$$

For two colloidal particles, such an interaction can be realized using optical tweezers [71] or an effective potential induced by feedback control [72]. Besides, it qualitatively mimics the interaction of trapped active particles studied in [72] or in a similar model [73].

Now imagine that an experimenter can operate a transformation of the Hamiltonian parameters with the goal to increase the strength of the local traps, but with a minimal energetic cost. That is, the boundaries of the transformation are $k_x(0) = k_y(0) < k_x(\tau) = k_y(\tau)$ while $a(0) = a(\tau)$ and $k_{\text{int}}(0) = k_{\text{int}}(\tau)$. We want to know the minimum dissipation that an experimenter can achieve for such a transformation. In the appendix C.1, we derive and compare the minimum dissipation protocols in the slow-driving limit for two paradigmatic cases: *i) partial control* in which the experimenter can only tune the values of k_x and k_y (while a and k_{int} are both constant), *ii) total control* in which the experimenter can control k_{int} and a as well. The comparison among the two situations is presented in figure 1. As expected, the dissipation under partial control, $W_{\text{irr}}^{\text{PC}}$, is always larger than that for total control, $W_{\text{irr}}^{\text{TC}}$. In particular we observe that having the possibility of controlling all the parameters of the potential (25) allows, in general, substantial savings of up to $\simeq 50\%$ of energy dissipation with respect to simply tuning the stiffnesses $k_{x,y}$.

5.2. Rotating a 2-dimensional squeezed potential

As a second example, we consider the rotation of a two-dimensional Gaussian system in the xy plane. Specifically, we consider a Gaussian PDF with a non-isotropic covariance matrix of the position coordinates $\{x, y\}$

$$\left(\begin{array}{cc} \langle x^2 \rangle & \langle xy \rangle \\ \langle xy \rangle & \langle y^2 \rangle \end{array} \right), \quad (26)$$

which is squeezed with the major axis and the x -axis forming an angle θ in the xy plane. Denoting the eigenvalues of Σ as ω_a and ω_b , it can be written in the form

$$\Sigma_{\theta, \omega_a, \omega_b} = \begin{pmatrix} \cos^2(\theta)\omega_a + \sin^2(\theta)\omega_b & \sin(\theta)\cos(\theta)(\omega_a - \omega_b) \\ \sin(\theta)\cos(\theta)(\omega_a - \omega_b) & \sin^2(\theta)\omega_a + \cos^2(\theta)\omega_b \end{pmatrix}. \quad (27)$$

Our goal is to find a minimum-dissipation protocol that would overall rotate the system in the xy plane, by an angle $\delta\theta = \frac{\pi}{4}$. We thus consider protocols starting at $\Sigma(0) = \Sigma_{0, \omega_a, \omega_b}$ and ending at $\Sigma(\tau) = \Sigma_{\frac{\pi}{4}, \omega_a, \omega_b}$ (cf figure 2), and compare three strategies for accomplishing this task: (i) Uniform rotation trajectory: the experimenter simply rotates the system, i.e., fixes the variances $\omega_{a,b}$ in Σ and increases θ ; (ii) Pseudo-commutative trajectory: the experimenter tunes $\omega_{a,b}$ to the same value at an intermediate time, thus making the distribution isotropic. Afterwards, they re-stretch the distribution in the desired direction. Such protocol satisfies $[\dot{\Sigma}(t), \Sigma(t)] = 0 \quad \forall t$ (notice however $[\Sigma(0), \Sigma(\tau)] \neq 0$, which implies Observation 1 cannot be applied in this case). The intermediate point can be chosen optimally to minimize the dissipation; (iii) Optimal protocol: the experimenter is able to control the system such that it follows the BW-geodesic $\bar{\Sigma}(t)$ in (14) between $\Sigma_{0, \omega_a, \omega_b}$ and $\Sigma_{\frac{\pi}{4}, \omega_a, \omega_b}$. Details of the calculations for each of the trajectories are given in appendix C.3 and the results are depicted in figure 2. We find that the pseudo-commutative strategy is strongly non-optimal, and dissipates at least twice as much as the geodesics trajectory. Notice that this is not in contradiction to Observation 1, as non-commuting boundary condition induce, in general, non-commuting optimal trajectories. At the same time we see that the uniform rotation of the system Σ is close to the optimal (geodesic) trajectory in terms of dissipation, while being simpler to implement (it corresponds to a rotation of the experimental apparatus with fixed traps' strength). Finally, no timescale approximation was used in this case, but we notice that in the slow-driving limit the above strategies are equivalently translated to the stiffness matrix $K = T\Sigma^{-1}$ (cf Observation 2).

6. Discussion

In this paper, we have studied the work, heat exchange, and irreversible work dissipation of overdamped multidimensional classical systems. These may have an arbitrary number of degrees of freedom and are confined by harmonic potentials whose parameters can be partially or totally controlled. Such systems are described by multidimensional Gaussian probability distributions [56]. For uniform friction and non-moving trap centers, we have derived a general analytic expression (9) for the irreversible work (proportional to the entropy production when the temperature is fixed). This expression is valid for any response trajectory, and allows geometric optimisation based on the Bures-Wasserstein metric for positive matrices. We also discussed straightforward generalizations of these results to non-uniform friction values and nontrivial trap center dynamics. Given that in the slow-driving limit there is a one-to-one mapping between the set of reachable states Σ and the set of reachable controls K , this further allows optimization of control protocols that incorporate experimental constraints, i.e., partial control. Finally, we described general design principles for optimal

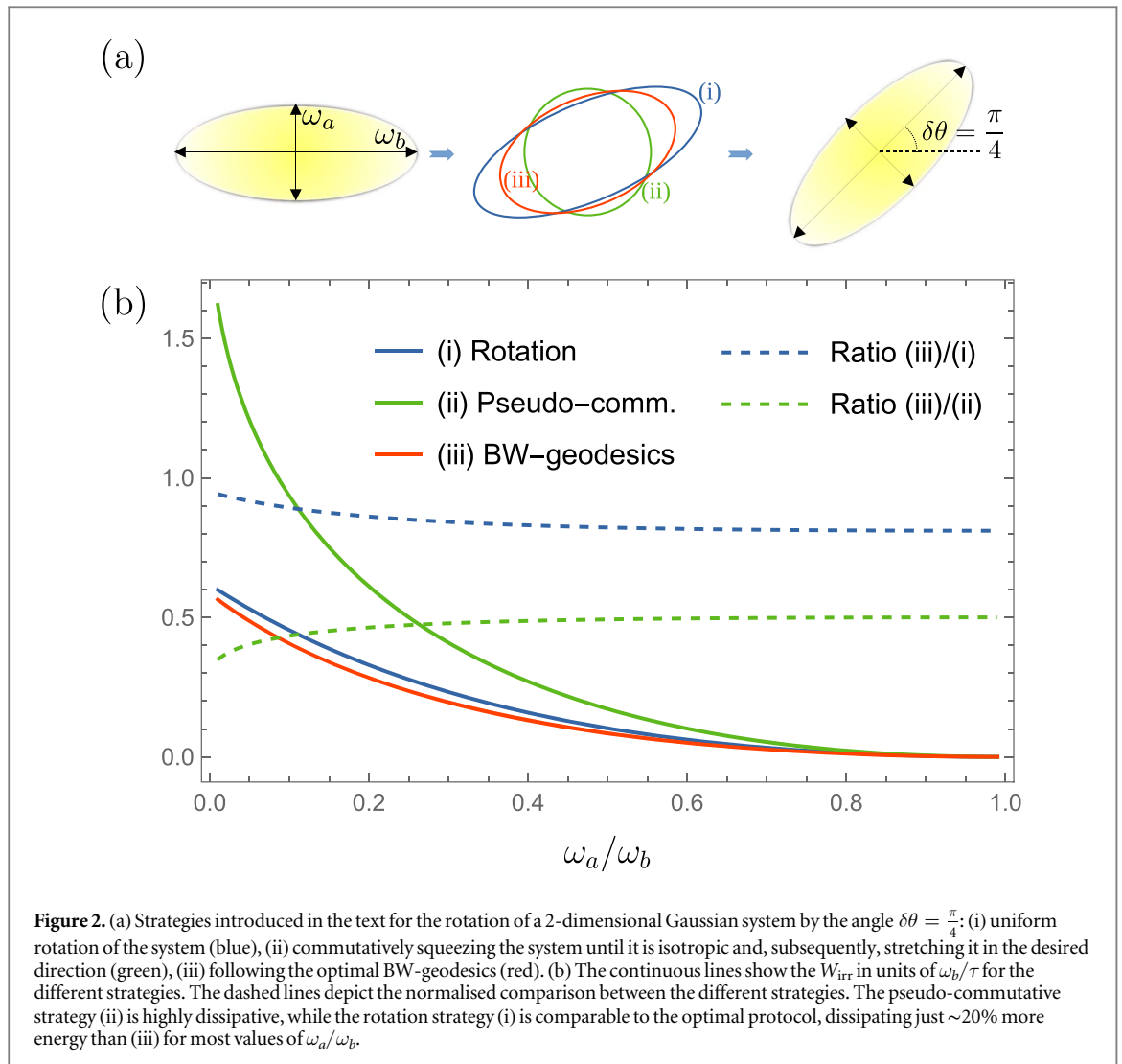


Figure 2. (a) Strategies introduced in the text for the rotation of a 2-dimensional Gaussian system by the angle $\delta\theta = \frac{\pi}{4}$: (i) uniform rotation of the system (blue), (ii) commutatively squeezing the system until it is isotropic and, subsequently, stretching it in the desired direction (green), (iii) following the optimal BW-geodesics (red). (b) The continuous lines show the W_{irr} in units of ω_b/τ for the different strategies. The dashed lines depict the normalised comparison between the different strategies. The pseudo-commutative strategy (ii) is highly dissipative, while the rotation strategy (i) is comparable to the optimal protocol, dissipating just $\sim 20\%$ more energy than (iii) for most values of ω_a/ω_b .

parameter protocols that minimise dissipation and illustrated them for two examples, increasing local confinement of two interacting particles and rotating a squeezed potential.

The obtained results point towards the manageable optimization of control protocols in experimental systems with many degrees of freedom [72, 73, 75–77], and they can be directly applied to optical tweezers setups and electric circuits [71, 78, 79], that wish to minimise dissipation by choosing optimised control parameter protocols. Moreover, our findings can be readily applied to the case of engines and refrigerators described in the low-dissipation regime, characterized by the $1/\tau$ scaling of dissipation [15, 32, 80–83]. Further extensions include the analysis of underdamped classical systems, as well as that of quantum Gaussian systems.

Acknowledgments

VH gratefully acknowledges support by the Humboldt foundation and by the Czech Science Foundation (project No. 20-02955J). PA is supported by ‘la Caixa’ Foundation (ID 100 010 434, Grant No. LCF/BQ/DI19/11730023), and by the Government of Spain (FIS2020-TRANQI and Severo Ochoa CEX2019-000910-S), Fundacio Cellex, Fundacio Mir-Puig, Generalitat de Catalunya (CERCA, AGAUR SGR 1381. FC gratefully acknowledges funding from the Foundational Questions Institute Fund (FQXi-IAF19-01). JA gratefully acknowledges funding from EPSRC (EP/R045577/1). ZY is grateful for the sponsorship of China Scholarship Council (CSC) under Grant No. 201 906 310 136. MPL acknowledges financial support from the Swiss National Science Foundation through an Ambizione grant PZ00P2-186067.

Data availability statement

All data that support the findings of this study are included within the article (and any supplementary files).

Appendix A. On the Bures-Wasserstein distance

The Bures-Wasserstein (BW) distance can be defined between positive semidefinite matrices $\Sigma \geq 0$, and its infinitesimal value is given by the metrics g_Σ

$$D_{\text{BW}}(\Sigma, \Sigma + d\Sigma)^2 = g_\Sigma(d\Sigma, d\Sigma) = \frac{1}{2} \int_0^\infty dv \text{Tr}[e^{-v\Sigma} d\Sigma e^{-v\Sigma} d\Sigma]. \quad (\text{A.1})$$

When applied to complex positive matrices of unit trace (that is, *states* in the field of quantum information), such metric represents a fundamental quantifier in problems of quantum statistical inference and metrology [57, 59, 61, 62]. At the same time it has its own relevance as a distance quantifier between positive real matrices or multivariate distributions, in the context of optimal transport theory [60, 63]. The integrated geodesics length between two points Σ_1 and Σ_2 , if no constraints are imposed on the trace of the matrices, reads

$$D_{\text{BW}}(\Sigma_1, \Sigma_2) = \sqrt{\text{Tr}[\Sigma_1] + \text{Tr}[\Sigma_2] - 2 \text{Tr}[\sqrt{\sqrt{\Sigma_1} \Sigma_2 \sqrt{\Sigma_1}}]} \quad (\text{A.2})$$

and the corresponding geodesics is

$$\Sigma(t) = (1-t)^2 \Sigma_1 + t^2 \Sigma_2 + t(1-t)(\sqrt{\Sigma_1 \Sigma_2} + \sqrt{\Sigma_2 \Sigma_1}) \quad (\text{A.3})$$

where the square root

$$\sqrt{\Sigma_1 \Sigma_2} = \Sigma_1^{\frac{1}{2}} (\Sigma_1^{\frac{1}{2}} \Sigma_2 \Sigma_1^{\frac{1}{2}})^{\frac{1}{2}} \Sigma_1^{-\frac{1}{2}} \quad (\text{A.4})$$

is the only matrix R satisfying $R^2 = \Sigma_1 \Sigma_2$ and having a positive spectrum (cf [60]).

Appendix B. General case and slow-driving solution

Here we consider the case in which also the first moment of the quadratic potential can be driven. We assume [56] that the state is Gaussian with covariance matrix $\Sigma(t)$ and first moments $\xi(t)$ (we avoid expliciting time when possible)

$$p(\mathbf{x}, t) = \frac{1}{\sqrt{(2\pi)^N \det \Sigma}} \exp\left(-\frac{(\mathbf{x} - \xi)^\top \Sigma^{-1} (\mathbf{x} - \xi)}{2}\right), \quad (\text{B.1})$$

while the potential is

$$V(\mathbf{x}, t) = \frac{1}{2} (\mathbf{x} - \mathbf{z}(t)) K(t) (\mathbf{x} - \mathbf{z}(t)), \quad (\text{B.2})$$

with $\xi \neq \mathbf{z}$ in general. The energy of the system is therefore

$$\begin{aligned} E(t) &= \int d\mathbf{x} p(\mathbf{x}, t) V(\mathbf{x}, t) \\ &= \frac{1}{2} \text{Tr}[\Sigma K] + \frac{1}{2} (\xi - \mathbf{z}) K (\xi - \mathbf{z}) = \frac{1}{2} \text{Tr}[\Sigma_z K], \end{aligned} \quad (\text{B.3})$$

where Σ_z is the covariance matrix *centered in z*, that is

$$\Sigma_z = \langle (\mathbf{x} - \mathbf{z})(\mathbf{x} - \mathbf{z})^\top \rangle = \Sigma + (\xi - \mathbf{z})(\xi - \mathbf{z})^\top. \quad (\text{B.4})$$

The Langevin equation (2) becomes accordingly $\dot{\mathbf{x}} = -K(\mathbf{x} - \mathbf{z}) + \sqrt{2T} \boldsymbol{\eta}$ in natural units, which is translated on the Gaussian moments as

$$\dot{\xi} = -K(\xi - \mathbf{z}), \quad (\text{B.5})$$

$$\partial_t \Sigma_z = -K \Sigma_z - \Sigma_z K + 2T, \quad (\text{B.6})$$

where the partial derivative in time is due to the fact that Σ_z depends as well on \mathbf{z} , i.e.

$$\dot{\Sigma}_z = \partial_t \Sigma_z - \dot{\mathbf{z}}(\xi - \mathbf{z})^\top - (\xi - \mathbf{z}) \dot{\mathbf{z}}^\top. \quad (\text{B.7})$$

The work and heat can be computed by simply taking the derivative w.r.t. the driving parameters K, \mathbf{z} (for the work), and the dynamical parameters Σ, ξ (for the heat), i.e.

$$\begin{aligned}
W &= \frac{1}{2} \int_0^\tau dt (\text{Tr}[\dot{K}\Sigma_z] + \partial_z \text{Tr}[K\Sigma_z]\dot{z}) \\
&= \frac{1}{2} \text{Tr}[K\Sigma_z] \Big|_0^\tau - \frac{1}{2} \int_0^\tau dt (\text{Tr}[K\dot{\Sigma}_z] - \partial_z \text{Tr}[K\Sigma_z]\dot{z}) \\
&= \frac{1}{2} \text{Tr}[K\Sigma_z] \Big|_0^\tau - \frac{1}{2} \int_0^\tau dt \text{Tr}[K\partial_t \Sigma_z].
\end{aligned} \tag{B.8}$$

Using the same steps as in the main text (integration by parts and equation (B.6)), this expression translates to

$$\begin{aligned}
W &= \frac{1}{2} \text{Tr}[K\Sigma_z] \Big|_0^\tau + \frac{T}{2} \int_0^\tau dt \text{Tr}[\Sigma_z^{-1} \partial_t \Sigma_z] \\
&\quad - \frac{1}{2} \int_0^\tau dt \text{Tr} \left[\int_0^\infty d\nu e^{-\nu \Sigma_z} \partial_t \Sigma_z e^{-\nu \Sigma_z} \partial_t \Sigma_z \right],
\end{aligned} \tag{B.9}$$

which can be rewritten as

$$\begin{aligned}
W &= \Delta E - \frac{T}{2} \Delta \det \Sigma_z \\
&= \frac{T}{2} \int_0^\tau dt \text{Tr}[\Sigma_z^{-1} (\dot{\Sigma}_z - \partial_t \Sigma_z)] + \int_0^\tau dt g_{\Sigma_z}(\partial_t \Sigma_z, \partial_t \Sigma_z),
\end{aligned} \tag{B.10}$$

with the BW metrics (10) g . Notice that in general $\frac{1}{2} \Delta \det \Sigma_z \neq \frac{1}{2} \Delta \det \Sigma = \Delta S$ and therefore the expression above cannot be identified as the irreversible work. At the same time, minimizing dissipation requires using finite time protocols in which the system ends in equilibrium with the thermal bath, so that no dissipation follows the end of the protocol. This is automatically satisfied in the case of slow-protocols (see below). For general transformations, it is sufficient to add a final quench of the controls, $(K(\tau), \mathbf{z}(\tau)) = (T\Sigma_z^{-1}(\tau), \boldsymbol{\xi}(\tau))$. The condition $\boldsymbol{\xi}(\tau) = \mathbf{z}(\tau)$ is sufficient to rewrite (B.10) as

$$W_{\text{irr}} = \frac{T}{2} \int_0^\tau dt \text{Tr}[\Sigma_z^{-1} (\dot{\Sigma}_z - \partial_t \Sigma_z)] + \int_0^\tau dt g_{\Sigma_z}(\partial_t \Sigma_z, \partial_t \Sigma_z), \tag{B.11}$$

which can be computed explicitly using $\partial_t \Sigma_z - \dot{\Sigma}_z = \dot{z}(\boldsymbol{\xi} - \mathbf{z})^\top + (\boldsymbol{\xi} - \mathbf{z})\dot{z}^\top$.

B.1. The slow case

In the slow-driving regime a first order expansion is performed around $\frac{1}{\tau} \simeq 0$ [68]. For example in the quasistatic limit of $\tau \rightarrow \infty$ the solution for the dynamics (B.5, B.6) is clearly $\boldsymbol{\xi}^{(0)} = \mathbf{z}$ and $\Sigma_z^{(0)} = \Sigma^{(0)} = TK^{-1}$. The finite time expansion leads to

$$\begin{aligned}
\boldsymbol{\xi} &= \boldsymbol{\xi}^{(0)} + \boldsymbol{\xi}^{(1)} + \boldsymbol{\xi}^{(2)} + \dots + \boldsymbol{\xi}^{(i)} \sim \mathcal{O}(\tau^{-i}) \\
\boldsymbol{\xi}^{(0)} &= \mathbf{z}, \quad \boldsymbol{\xi}^{(1)} = -K^{-1}\dot{z}.
\end{aligned} \tag{B.12}$$

As $\boldsymbol{\xi} - \mathbf{z} = -K^{-1}\dot{z} + \mathcal{O}(\tau^{-2})$, we also get

$$\Sigma_z = \Sigma + \dot{z}K^{-2}\dot{z}^\top + \mathcal{O}(\tau^{-3}), \tag{B.13}$$

$$\dot{\Sigma}_z - \partial_t \Sigma_z = \{\dot{z}\dot{z}^\top, K^{-1}\} + \mathcal{O}(\tau^{-3}) = \{\dot{\boldsymbol{\xi}}\dot{\boldsymbol{\xi}}^\top, K^{-1}\} + \mathcal{O}(\tau^{-3}). \tag{B.14}$$

Using the above expressions, the irreversible work reads

$$W_{\text{irr}} = \int_0^\tau dt (|\dot{\boldsymbol{\xi}}|^2 + g_\Sigma(\dot{\Sigma}, \dot{\Sigma})) + \mathcal{O}(\tau^{-2}) \tag{B.15}$$

$$= \int_0^\tau dt (|\dot{z}|^2 + Tg_{K^{-1}}(\dot{K}^{-1}, \dot{K}^{-1})) + \mathcal{O}(\tau^{-2}). \tag{B.16}$$

Appendix C. Detailed and solved examples

C.1. Double trap

Consider the potential

$$V = \frac{1}{2}k_x \left(x - \frac{a}{2}\right)^2 + \frac{1}{2}k_y \left(y + \frac{a}{2}\right)^2 + \frac{1}{2}k_{\text{int}}(x - y)^2, \tag{C.1}$$

which can be rewritten in matrix form as

$$V = \frac{1}{2}(\mathbf{x} - \mathbf{a})^\top K(\mathbf{x} - \mathbf{a}) + \frac{1}{2}\mathbf{x}^\top K_{\text{int}}\mathbf{x} \tag{C.2}$$

with

$$\mathbf{x} = \begin{pmatrix} x \\ y \end{pmatrix}, \mathbf{a} = \begin{pmatrix} a/2 \\ -a/2 \end{pmatrix}, K = \begin{pmatrix} k_x & 0 \\ 0 & k_y \end{pmatrix}, K_{\text{int}} = \begin{pmatrix} k_{\text{int}} & -k_{\text{int}} \\ -k_{\text{int}} & k_{\text{int}} \end{pmatrix}. \quad (\text{C.3})$$

To use equation (19), we rewrite the potential in the ‘canonical form’

$$V = \frac{1}{2}(\mathbf{x} - \mathbf{a}')^\top (K + K_{\text{int}})(\mathbf{x} - \mathbf{a}') - \frac{1}{2}\mathbf{a}'^\top (K + K_{\text{int}})\mathbf{a}' + \frac{1}{2}\mathbf{a}'^\top K\mathbf{a}, \quad (\text{C.4})$$

where

$$\mathbf{a}' = (K + K_{\text{int}})^{-1}K\mathbf{a} \quad (\text{C.5})$$

is the effective center of the potential. The scalar $-\frac{1}{2}\mathbf{a}'^\top (K + K_{\text{int}})\mathbf{a}' + \frac{1}{2}\mathbf{a}'^\top K\mathbf{a}$ is just a global shift in energy that does not depend on the dynamics of the system and vanishes for cyclic protocols.

C.2. Confining the particles—Irreversibility parameter

We compute the irreversible work using the slow-driving approximation equation (19), in which the center of the distribution can be substituted by the center of the potential, and the covariance matrix can be substituted by the inverse stiffness matrix (cf appendix B), leading to

$$W_{\text{irr}} = \int_0^\tau dt (|\dot{\mathbf{a}}'|^2 + g_\Sigma(\dot{\Sigma}, \dot{\Sigma})) \quad \text{with} \quad \Sigma = T(K + K_{\text{int}})^{-1}. \quad (\text{C.6})$$

Suppose the experimenter wants increase the strength of the local traps to increase the confinement of the two particles. The endpoint of the transformation will therefore be

$$a(0) = a(\tau), k_{\text{int}}(0) = k_{\text{int}}(\tau), k_x(0) = k_y(0) < k_x(\tau) = k_y(\tau). \quad (\text{C.7})$$

We notice that due to the symmetry of the potential at the boundary, the eigenvectors of $K + K_{\text{int}}$ are always (1, 1) and (1, -1), independently of the values of k_{int} and $k_x=k_y$. That is, $[(K + K_{\text{int}})(0), (K + K_{\text{int}})(\tau)] = 0$ and we can therefore assume that it commutes with itself at all times (cf Observation 1). In such case, the contribution of $g_\Sigma(\dot{\Sigma}, \dot{\Sigma})$ to W_{irr} simplifies to (cf equation (16))

$$g_\Sigma(\dot{\Sigma}, \dot{\Sigma}) = \frac{1}{2} \int_0^\tau dt \text{Tr} \left[\int_0^\infty d\nu e^{-\nu\Sigma\dot{\Sigma}} e^{-\nu\Sigma\dot{\Sigma}} \right] = \frac{1}{4} \left(\frac{\dot{\omega}_1^2}{\omega_1} + \frac{\dot{\omega}_2^2}{\omega_2} \right), \quad (\text{C.8})$$

where ω_i are the eigenvalues of $\Sigma = T(K + K_{\text{int}})^{-1}$, which are easily computed. In particular given $k_x = k_y \equiv k$ we have

$$\omega_1 = \frac{T}{k}, \quad \omega_2 = \frac{T}{k + 2k_{\text{int}}}, \quad (\text{C.9})$$

and therefore

$$g_\Sigma(\dot{\Sigma}, \dot{\Sigma}) = \frac{T}{4} \left(\frac{\dot{k}^2}{k^3} + \frac{(\dot{k} + 2\dot{k}_{\text{int}})^2}{(k + 2k_{\text{int}})^3} \right). \quad (\text{C.10})$$

The contribution $|\dot{\mathbf{a}}'|^2$ to W_{irr} follows from equation (C.5):

$$\mathbf{a}' = \frac{k}{k + 2k_{\text{int}}} \frac{a}{2} \begin{pmatrix} 1 \\ -1 \end{pmatrix} \quad (\text{C.11})$$

$$|\dot{\mathbf{a}}'|^2 = 2a^2 \left(\frac{k}{k + 2k_{\text{int}}} \right)^4 \left(\frac{d}{dt} \left(\frac{k_{\text{int}}}{k} \right) \right)^2 + \frac{\dot{a}^2}{2} \left(\frac{k}{k + 2k_{\text{int}}} \right)^2. \quad (\text{C.12})$$

The associated dissipation of the transformation can be computed from the expressions above for any slow transformation. We now consider the *partial control* (PC) case in which the distance a and interaction strength k_{int} is fixed, and the experimenter can only control the local stiffnesses $k_x = k_y \equiv k$. Substituting (C.10) and (C.12) with $\dot{a} = \dot{k}_{\text{int}} = 0$, the irreversible work (C.6) then specifies to

$$\dot{W}_{\text{irr}} = \frac{T}{4} \left(\frac{1}{k^3} + \frac{1}{(k + 2k_{\text{int}})^3} \right) \dot{k}^2 + 2a^2 \frac{k_{\text{int}}^2}{(k + 2k_{\text{int}})^4} \dot{k}^2. \quad (\text{C.13})$$

For fixed boundary values of k , it can be proven using the Cauchy-Schwarz inequality that the dissipation with partial control (C.13) is lower-bounded by

$$W_{\text{irr}}^{\text{PC}} \geq \frac{1}{\tau} \left(\int_{k_1}^{k_2} dk \sqrt{\frac{T}{4} \left(\frac{1}{k^3} + \frac{1}{(k+2k_{\text{int}})^3} \right) + 2a^2 \frac{k_{\text{int}}^2}{(k+2k_{\text{int}})^4}} \right)^2. \quad (\text{C.14})$$

By comparison, in the case of *total control* (TC), the bound for the dissipation is given by (20), which, in our case, reads

$$W_{\text{irr}}^{\text{TC}} \geq \frac{1}{\tau} (|\mathbf{a}'_1 - \mathbf{a}'_2|^2 + D_{\text{BW}}(\Sigma_1, \Sigma_2)^2), \quad \text{with} \quad (\text{C.15})$$

$$|\mathbf{a}'_1 - \mathbf{a}'_2|^2 = \frac{a^2}{2} \left(\frac{k_1}{k_1 + 2k_{\text{int}}} - \frac{k_2}{k_2 + 2k_{\text{int}}} \right)^2, \quad (\text{C.16})$$

$$\frac{D_{\text{BW}}(\Sigma_1, \Sigma_2)^2}{T} = \left(\frac{1}{\sqrt{k_1}} - \frac{1}{\sqrt{k_2}} \right)^2 + \left(\frac{1}{\sqrt{k_1 + 2k_{\text{int}}}} - \frac{1}{\sqrt{k_2 + 2k_{\text{int}}}} \right)^2. \quad (\text{C.17})$$

C.3. Rotating a 2-dimensional system

In this section, we consider the rotation of a covariance matrix Σ in 2 dimensions by an angle $\theta = \frac{\pi}{4}$. We thus impose the boundary conditions

$$\Sigma_{\text{in}} = \begin{pmatrix} \omega_a & 0 \\ 0 & \omega_b \end{pmatrix}, \quad \Sigma_{\text{fin}} = \frac{1}{2} \begin{pmatrix} \omega_a + \omega_b & \omega_a - \omega_b \\ \omega_a - \omega_b & \omega_a + \omega_b \end{pmatrix}. \quad (\text{C.18})$$

And we minimize the irreversible work (9) according to three possible strategies.

C.3.1. Simple rotation protocol. First, we consider the transformation from Σ_{in} to Σ_{fin} to be performed by uniformly rotating the experimental apparatus, without modifying the squeezing $\{\omega_a, \omega_b\}$ of the distribution. This corresponds to an angle-parametrized protocol

$$\Sigma_{\theta} = \begin{pmatrix} \cos^2(\theta)\omega_a + \sin^2(\theta)\omega_b & \sin(\theta)\cos(\theta)(\omega_a - \omega_b) \\ \sin(\theta)\cos(\theta)(\omega_a - \omega_b) & \sin^2(\theta)\omega_a + \cos^2(\theta)\omega_b \end{pmatrix} \quad (\text{C.19})$$

starting at $\Sigma_0 \equiv \Sigma_{\text{in}}$ and ending at $\Sigma_{\frac{\pi}{4}} \equiv \Sigma_{\text{fin}}$. The irreversible work production (9) is in this case given by $W_{\text{irr}} = \frac{1}{2} \int_0^{\tau} dt \text{Tr} \left[\int_0^{\infty} d\nu e^{-\nu\Sigma} \dot{\Sigma} e^{-\nu\Sigma} \dot{\Sigma} \right]$. Given the rotational symmetry of the problem, it is obvious that the optimal rotation of the system will have a constant speed $\dot{\theta}$. Thus the integrand

$$\dot{W}_{\text{irr}} = \frac{1}{2} \text{Tr} \left[\int_0^{\infty} d\nu e^{-\nu\Sigma} \dot{\Sigma} e^{-\nu\Sigma} \dot{\Sigma} \right] \quad (\text{C.20})$$

will be constant in time and can be computed, e.g., for $\theta = 0$, which yields

$$\Sigma = \begin{pmatrix} \omega_a & 0 \\ 0 & \omega_b \end{pmatrix}, \quad \dot{\Sigma} = \dot{\theta} \begin{pmatrix} 0 & \omega_a - \omega_b \\ \omega_a - \omega_b & 0 \end{pmatrix}. \quad (\text{C.21})$$

Now we use the fact that the operator $\mathcal{I}(A, B) = \int_0^{\infty} d\nu e^{-\nu A} B e^{-\nu A}$ can be easily expressed in components as $\mathcal{I}(A, B)_{ij} = \frac{B_{ij}}{a_i + a_j}$, in the basis that diagonalizes A , i.e., $A_{ij} = \delta_{ij} a_i$. We therefore get

$$\int_0^{\infty} d\nu e^{-\nu\Sigma} \dot{\Sigma} e^{-\nu\Sigma} = \dot{\theta} \frac{\omega_a - \omega_b}{\omega_a + \omega_b} \begin{pmatrix} 0 & 1 \\ 1 & 0 \end{pmatrix}, \quad (\text{C.22})$$

from which it is easy to compute the value of (C.20):

$$\dot{W}_{\text{irr}} = \dot{\theta}^2 \frac{(\omega_a - \omega_b)^2}{\omega_a + \omega_b}. \quad (\text{C.23})$$

The minimum value of $W_{\text{irr}} = \int_0^{\tau} \dot{W}_{\text{irr}}$ for the uniform rotation over the total angle $\Delta\theta = \frac{\pi}{4}$ is thus given by

$$W_{\text{irr}} = \frac{1}{\tau} \frac{\pi^2}{16} \frac{(\omega_a - \omega_b)^2}{\omega_a + \omega_b}. \quad (\text{C.24})$$

C.3.2. Pseudo-commutative protocol. One possible way to interpolate between Σ_{in} and Σ_{fin} (C.18) is to change the values of $\omega_{a,b}$ to reach an intermediate symmetric covariance matrix

$$\Sigma_{\text{intermediate}} = \begin{pmatrix} \omega_c & 0 \\ 0 & \omega_c \end{pmatrix}, \quad (\text{C.25})$$

which is proportional to the identity matrix, and later ‘re-stretch’ it in the $\pi/4$ direction in the same way. Such protocol is *locally commutative* at all times, in the sense that $[\Sigma(t), \dot{\Sigma}(t)] = 0 \quad \forall t$, although the final and initial covariance matrices do not commute. The total irreversible work for such a strategy is clearly twice the

irreversible work obtained for the transformation $\Sigma_{\text{in}} \rightarrow \Sigma_{\text{intermediate}}$, in a time $\tau/2$. We therefore get, using the commutative result (16),

$$W_{\text{irr}} = \frac{4}{\tau} ((\sqrt{\omega_a} - \sqrt{\omega_c})^2 + (\sqrt{\omega_b} - \sqrt{\omega_c})^2). \quad (\text{C.26})$$

ω_c is a free parameter of the described protocol, which can be chosen to minimize W_{irr} . The optimal choice is $\omega_c = \left(\frac{\sqrt{\omega_a} + \sqrt{\omega_b}}{2}\right)^2$, leading to the minimum dissipation for pseudo-commutative protocols

$$W_{\text{irr}} = \frac{2}{\tau} (\sqrt{\omega_a} - \sqrt{\omega_b})^2. \quad (\text{C.27})$$

C.4. Optimal protocol

The minimal value of dissipation for any protocol between Σ_{in} and Σ_{fin} is given by the main lower bound (12), which is saturated when performing the BW-geodesics (14). In our case, we obtain

$$\begin{aligned} \frac{D_{\text{BW}}(\Sigma_{\text{in}}, \Sigma_{\text{fin}})^2}{\tau} &= \frac{1}{\tau} (\text{Tr}[\Sigma_{\text{in}}] + \text{Tr}[\Sigma_{\text{fin}}] - 2 \text{Tr}[\sqrt{\Sigma_{\text{in}} \Sigma_{\text{fin}} \Sigma_{\text{in}}}]) \\ &= \frac{1}{\tau} (2(\omega_a + \omega_b) - \sqrt{2} \sqrt{2(\omega_a + \omega_b)^2 - (\omega_a - \omega_b)^2}). \end{aligned} \quad (\text{C.28})$$

ORCID iDs

Paolo Abiuso  <https://orcid.org/0000-0001-5019-7823>

Viktor Holubec  <https://orcid.org/0000-0002-6576-1316>

Martí Perarnau-Llobet  <https://orcid.org/0000-0002-4658-0632>

References

- [1] Andresen B, Salamon P and Berry R S 1984 Thermodynamics in finite time *Physics Today* **37** 62–70
- [2] Andresen B, Berry R S, Ondrechen M J and Salamon P 1984 Thermodynamics for processes in finite time *Acc. Chem. Res.* **17** 266–71
- [3] Defnner S and Bonança M V S 2020 Thermodynamic control—an old paradigm with new applications *EPL* **131** 20001
- [4] Seifert U 2012 Stochastic thermodynamics, fluctuation theorems and molecular machines *Rep. Prog. Phys.* **75** 126001
- [5] Myers N M, Abah O and Defnner S 2022 Quantum thermodynamic devices: from theoretical proposals to experimental reality *AVS Quantum Sci.* **4** 027101
- [6] Zulkowski P R and DeWeese M R 2014 Optimal finite-time erasure of a classical bit *Phys. Rev. E* **89** 052140
- [7] Proesmans K, Ehrich J and Bechhoefer J 2020 Finite-time landauer principle *Phys. Rev. Lett.* **125** 100602
- [8] Zhen Y-Z, Egloff D, Modi K and Dahlsten O 2021 Universal bound on energy cost of bit reset in finite time *Phys. Rev. Lett.* **127** 190602
- [9] Jarzynski C 1997 Nonequilibrium equality for free energy differences *Phys. Rev. Lett.* **78** 2690
- [10] Sekimoto K 1998 L equation and thermodynamics *Prog. Theor. Phys. Suppl.* **130** 17–27
- [11] Crooks G E 1999 Entropy production fluctuation theorem and the nonequilibrium work relation for free energy differences *Phys. Rev. E* **60** 2721
- [12] Seifert U 2005 Entropy production along a stochastic trajectory and an integral fluctuation theorem *Phys. Rev. Lett.* **95** 040602
- [13] Jarzynski C 2011 Equalities and inequalities: Irreversibility and the second law of thermodynamics at the nanoscale *Annu. Rev. Condens. Matter Phys.* **2** 329–51
- [14] Miller H J D and Anders J 2017 Entropy production and time asymmetry in the presence of strong interactions *Phys. Rev. E* **95** 062123
- [15] Schmiedl T and Seifert U 2007 Optimal finite-time processes in stochastic thermodynamics *Phys. Rev. Lett.* **98** 108301
- [16] Schmiedl T and Seifert U 2007 Efficiency at maximum power: An analytically solvable model for stochastic heat engines *EPL (Europhysics Letters)* **81** 20003
- [17] Holubec V 2014 An exactly solvable model of a stochastic heat engine: optimization of power, power fluctuations and efficiency *J. Stat. Mech: Theory Exp.* **2014** P05022
- [18] Plata C A, Guéry-Odelin D, Trizac E and Prados A 2019 Optimal work in a harmonic trap with bounded stiffness *Phys. Rev. E* **99** 012140
- [19] Zhang Y 2020 Optimization of stochastic thermodynamic machines *J. Stat. Phys.* **178** 1336–53
- [20] Miangolarra O M, Taghvaei A, Fu R, Yo Chen and Georgiou T T 2021 Energy harvesting from anisotropic fluctuations *Phys. Rev. E* **104** 044101
- [21] Gomez-Marin A, Schmiedl T and Seifert U 2008 Optimal protocols for minimal work processes in underdamped stochastic thermodynamics *J. Chem. Phys.* **129** 024114
- [22] Dechant A, Kiesel N and Lutz E 2017 Underdamped stochastic heat engine at maximum efficiency *EPL* **119** 50003
- [23] Miangolarra O M, Fu R, Taghvaei A, Chen Y and Georgiou T T 2021 Underdamped stochastic thermodynamic engines in contact with a heat bath with arbitrary temperature profile *Phys. Rev. E* **103** 062103
- [24] Esposito M, Kawai R, Lindenberg K and Van den Broeck C 2010 Finite-time Thermodynamics for A Single-Level Quantum Dot *EPL* **89** 20003
- [25] Ruppeiner G 1995 Riemannian geometry in thermodynamic fluctuation theory *Rev. Mod. Phys.* **67** 605–59
- [26] Salamon P and Berry R S 1983 Thermodynamic length and dissipated availability *Phys. Rev. Lett.* **51** 1127–30
- [27] Nulton J, Salamon P, Andresen B and Anmin Q 1985 Quasistatic processes as step equilibrations *J. Chem. Phys.* **83** 334–8
- [28] Crooks G E 2007 Measuring thermodynamic length *Phys. Rev. Lett.* **99** 100602
- [29] Sivak D A and Crooks G E 2012 Thermodynamic metrics and optimal paths *Phys. Rev. Lett.* **108** 190602
- [30] Zulkowski P R, Sivak D A, Crooks G E and DeWeese M R 2012 Geometry of thermodynamic control *Phys. Rev. E* **86** 041148

- [31] Bonança M V S and Deffner S 2014 Optimal driving of isothermal processes close to equilibrium *J. Chem. Phys.* **140** 244119
- [32] Abiuso P, Miller H J D, Perarnau-Llobet M and Scandi M 2020 Geometric optimisation of quantum thermodynamic processes *Entropy* **22** 1076
- [33] Rotskoff G M and Crooks G E 2015 Optimal control in nonequilibrium systems: Dynamic riemannian geometry of the ising model *Phys. Rev. E* **92** 060102
- [34] Gingrich T R, Rotskoff G M, Crooks G E and Geissler P L 2016 Near-optimal protocols in complex nonequilibrium transformations *PNAS* **113** 10263–8
- [35] Rotskoff G M, Crooks G E and Vanden-Eijnden E 2017 Geometric approach to optimal nonequilibrium control: Minimizing dissipation in nanomagnetic spin systems *Phys. Rev. E* **95** 012148
- [36] Scandi M and Perarnau-Llobet M 2019 Thermodynamic length in open quantum systems *Quantum* **3** 197
- [37] Abiuso P and Perarnau-Llobet M 2020 Optimal cycles for low-dissipation heat engines *Phys. Rev. Lett.* **124** 110606
- [38] Brandner K and Saito K 2020 Thermodynamic geometry of microscopic heat engines *Phys. Rev. Lett.* **124** 040602
- [39] Miller H J D and Mehboudi M 2020 Geometry of work fluctuations versus efficiency in microscopic thermal machines *Phys. Rev. Lett.* **125** 260602
- [40] Bhandari B, Alonso P T, Taddei F, von Oppen F, Fazio R and Arrachea L 2020 Geometric properties of adiabatic quantum thermal machines *Phys. Rev. B* **102** 155407
- [41] Terrén Alonso P, Abiuso P, Perarnau-Llobet M and Arrachea L 2022 Geometric optimization of nonequilibrium adiabatic thermal machines and implementation in a qubit system *PRX Quantum* **3** 010326
- [42] Frim A G and DeWeese M R 2021 Optimal finite-time brownian carnot engine arXiv:2107.05673
- [43] Frim A G and DeWeese M R 2021 A geometric bound on the efficiency of irreversible thermodynamic cycles arXiv:2112.10797
- [44] Eglinton J and Brandner K 2022 Geometric bounds on the power of adiabatic thermal machines arXiv:2202.08759
- [45] Cavina V, Erdman P A, Abiuso P, Tolomeo L and Giovannetti V 2021 Maximum-power heat engines and refrigerators in the fast-driving regime *Phys. Rev. A* **104** 032226
- [46] Erdman P A, Cavina V, Fazio R, Taddei F and Giovannetti V 2019 Maximum power and corresponding efficiency for two-level heat engines and refrigerators: optimality of fast cycles *New J. Phys.* **21** 103049
- [47] Das A and Mukherjee V 2020 Quantum-enhanced finite-time otto cycle *Phys. Rev. Research* **2** 033083
- [48] Blaber S, Louwerse M D and Sivak D A 2021 Steps minimize dissipation in rapidly driven stochastic systems *Phys. Rev. E* **104** L022101
- [49] Aurell E, Mejía-Monasterio C and Muratore-Ginanneschi P 2011 Optimal protocols and optimal transport in stochastic thermodynamics *Phys. Rev. Lett.* **106** 250601
- [50] Aurell E, Gawedzki K, Mejía-Monasterio C, Mohayae R and Muratore-Ginanneschi P 2012 Refined second law of thermodynamics for fast random processes *J. Stat. Phys.* **147** 487–505
- [51] Dechant A and Sakurai Y 2019 Thermodynamic interpretation of wasserstein distance arXiv:1912.08405
- [52] Chen Y, Georgiou T T and Tannenbaum A 2019 Stochastic control and nonequilibrium thermodynamics: Fundamental limits *IEEE Trans. Autom. Control* **65** 2979–91
- [53] Van Vu T and Hasegawa Y 2021 Geometrical bounds of the irreversibility in markovian systems *Phys. Rev. Lett.* **126** 010601
- [54] Nakazato M and Ito S 2021 Geometrical aspects of entropy production in stochastic thermodynamics based on wasserstein distance *Phys. Rev. Research* **3** 043093
- [55] Dechant A 2021 Minimum entropy production, detailed balance and wasserstein distance for continuous-time markov processes arXiv:2110.01141
- [56] Risken H 1996 Fokker-planck equation *In The Fokker-Planck Equation* (Berlin: Springer) pp 63–95
- [57] Paris M G A 2009 Quantum estimation for quantum technology *International Journal of Quantum Information* **7** 125–37
- [58] Sekimoto K 2010 *Stochastic Energetics* vol 799 (Berlin: Springer)
- [59] Bengtsson I and Życzkowski K 2017 *Geometry of Quantum States: An Introduction To Quantum Entanglement* (Cambridge: Cambridge University Press)
- [60] Bhatia R, Jain T and Lim Y 2019 On the bures-wasserstein distance between positive definite matrices *Expositiones Mathematicae* **37** 165–91
- [61] Wootters W K 1981 Statistical distance and hilbert space *Phys. Rev. D* **23** 357
- [62] Braunstein S L and Caves C M 1994 Statistical distance and the geometry of quantum states *Phys. Rev. Lett.* **72** 3439
- [63] Olkin I and Pukelsheim F 1982 The distance between two random vectors with given dispersion matrices *Linear Algebr. Appl.* **48** 257–63
- [64] Nakazato M and Ito S 2021 Geometrical aspects of entropy production in stochastic thermodynamics based on wasserstein distance *Phys. Rev. Research* **3** 043093
- [65] Bauer M, Brandner K and Seifert U 2016 Optimal performance of periodically driven, stochastic heat engines under limited control *Phys. Rev. E* **93** 042112
- [66] Ye Z, Cerisola F, Abiuso P, Anders J, Perarnau-Llobet M and Holubec V 2022 Optimal finite-time heat engines under constrained control arXiv:2202.12953
- [67] Zhong A and DeWeese M R 2022 Limited-control optimal protocols arbitrarily far from equilibrium arXiv:2205.08662
- [68] Cavina V, Mari A and Giovannetti V 2017 Slow dynamics and thermodynamics of open quantum systems *Phys. Rev. Lett.* **119** 050601
- [69] Brandner K, Saito K and Seifert U 2015 Thermodynamics of micro- and nano-systems driven by periodic temperature variations *Phys. Rev. X* **5** 031019
- [70] Brandner K and Seifert U 2016 Periodic thermodynamics of open quantum systems *Phys. Rev. E* **93** 062134
- [71] Jones P H, Maragò O M and Volpe G 2015 *Optical Tweezers: Principles and Applications* (Cambridge: Cambridge University Press)
- [72] Khadka U, Holubec V, Yang H and Cichos F 2018 Active particles bound by information flows *Nat. Commun.* **9** 3864
- [73] Krishnamurthy S, Ganapathy R and Sood A K 2021 Synergistic action in colloidal heat engines coupled by non-conservative flows arXiv:2101.07015
- [74] Mamede I N, Harunari P E, Akasaki B A N, Proesmans K and Fiore C E 2022 Obtaining efficient thermal engines from interacting brownian particles under time-periodic drivings *Phys. Rev. E* **105** 024106
- [75] Hucul D, Yeo M, Olmschenk S, Monroe C, Hensinger W K and Rabchuk J 2008 On the transport of atomic ions in linear and multidimensional ion trap arrays *Quantum Information & Computation* **8** 501–78
- [76] Renaut C, Cluzel B, Dellinger J, Lalouat L, Picard E, Peyrade D, Hadji E and De Fornel F 2013 On chip shapeable optical tweezers *Sci. Rep.* **3** 1–4
- [77] Mayer D, Schmidt F, Haupt S, Bouton Q, Adam D, Lausch T, Lutz E and Widera A 2020 Nonequilibrium thermodynamics and optimal cooling of a dilute atomic gas *Phys. Rev. Research* **2** 023245

- [78] Ciliberto S 2017 Experiments in stochastic thermodynamics: Short history and perspectives *Phys. Rev. X* **7** 021051
- [79] Gao D, Ding W, Nieto-Vesperinas M, Ding X, Rahman M, Zhang T, Lim C and Qiu C-W 2017 Optical manipulation from the microscale to the nanoscale: fundamentals, advances and prospects *Light: Science & Applications* **6** e17039
- [80] Esposito M, Kawai R, Lindenberg K and Van den Broeck C 2010 Efficiency at maximum power of low-dissipation carnot engines *Phys. Rev. Lett.* **105** 150603
- [81] Martínez I A, Roldán É, Dinis L, Petrov D, Parrondo J M R and Rica R A 2015 Brownian carnot engine *Nat. Phys.* **12** 67–70
- [82] Ma Y, Xu D, Dong H and Sun C-P 2018 Universal constraint for efficiency and power of a low-dissipation heat engine *Phys. Rev. E* **9** 042112
- [83] Ye Z and Holubec V 2021 Maximum efficiency of absorption refrigerators at arbitrary cooling power *Phys. Rev. E* **103** 052125